Radiochim. Acta **91**, 751–760 (2003)

Thermodynamic model for the solubility of ThO_2(am) in the aqueous Na^+-H^+-OH^--NO_3^--H_2O-EDTA system

By Yuanxian Xia[1,*], Andrew R. Felmy[1], Linfeng Rao[2], Zheming Wang[1] and Nancy J. Hess[1]

[1] Pacific Northwest National Laboratory, Richland, WA 99352, USA
[2] Lawrence Berkeley National Laboratory, Berkeley, CA 94720, USA

(Received March 7, 2003; accepted in final form June 9, 2003)

Solubility / Thorium complexes / EDTA complexes / Thermodynamic data / Pitzer model / Ion-interaction parameters

Summary. The solubility of ThO_2(am) in the aqueous Na^+-H^+-OH^--NO_3^--H_2O-EDTA system as a function of pC_{H^+} ($= -\log[H^+]$) and variable $NaNO_3$ (0.5 M to 6.0 M) has been determined. The experimental observations show that between pC_{H^+} values 4.2 to 8.2, a stoichiometric 1 : 1 Th-EDTA complex forms that completely saturates the added chelate concentration. Th concentrations then decrease linearly with increasing pC_{H^+} at $pC_{H^+} > 9.0$. These changes in solubility are not predicted by currently available thermodynamic models. The ion-interaction model of Pitzer was used to interpret these solubility data. Thermodynamic analysis indicates that the speciation under basic conditions is dominated by monomeric mixed Th-OH-EDTA complexes. X-ray absorption near-edge spectroscopy confirmed the absence of the higher order (*e.g.* dimeric) species. The equilibrium constants for the following reactions were determined from analysis of the solubility data: $ThO_2(am) + EDTA^{4-} + 2H_2O \leftrightarrow Th(OH)_2EDTA^{2-} + 2OH^-$, $\log K = -6.0$; and $ThO_2(am) + EDTA^{4-} + 2H_2O \leftrightarrow Th(OH)_3EDTA^{3-} + OH^-$, $\log K \sim -7.5$. Pitzer ion-interaction parameters for the $Th(OH)_2EDTA^{2-}$ and the $Th(OH)_3EDTA^{3-}$ species were calculated.

It was also determined that the solubility method for examining the complexation of tetravalent actinides with EDTA is limited to relatively high aqueous EDTA concentrations, relative to the amount of ThO_2(am) precipitate, owing to the adsorption of the EDTA chelator by the solid phase.

Introduction

High-level radioactive waste tanks at U.S. Department of Energy (DOE) storage sites have been found to leak highly basic, high ionic strength, waste solutions into the subsurface. These wastes contained, or are suspected to have contained, significant concentrations of radioactive species, including actinides. Several of these tanks also contain significant concentrations of organic chelating agents including EDTA, N-(2-hydroxyethyl) ethylenedinitrilotriacetic acid (HEDTA), and nitrilotriacetic acid (NTA). These chelating agents have the capability of complexing actinide species and other elements and transporting them through the subsurface in the vicinity of a tank leak. In addition, these chelating agents can affect processing strategies designed to remove hazardous radionuclides, including actinides, from the tanks waste supernatants [1].

Among the contaminants, tetravalent actinides (An(IV)) are expected to be important in these high-level nuclear wastes. Although tetravalent actinides readily form solid phases that are very insoluble when compared with the penta- and hexavalent states, An(IV) species can also form much stronger complexes with organic chelates [2, 3]. The complexation of An(IV) species with chelating agents stabilizes the An(IV) in soluble forms that may increase their migration potential in the subsurface and affect tank-processing strategies designed to remove these elements.

In order to be able to assess the effects of release of the long-lived actinide elements into the environment from such tank wastes, it is necessary to understand the chemistry under the conditions likely to be encountered. In particular, because concentrated $NaNO_3$ and high base solutions may exist in tank wastes, studies of the chemical behavior of actinides in these solutions are of importance.

It is well known that several actinides, especially neptunium and plutonium, are among the elements that exhibit the most versatile redox chemistry [4]. Depending on the solution conditions, they can exist in oxidation states ranging from III to VII, and several oxidation states of the same element (*e.g.*, Pu(III) to Pu(VI)) can exist simultaneously in significant amounts in solution. Np(IV) is redox sensitive and can be easily oxidized to Np(V), and thus, for Pu(IV) and Np(IV), special precautions must be taken to maintain their tetravalent oxidation states during the preparation of stock solutions of Np(IV) and Pu(IV) and throughout the solvent extraction and solubility experiments [3, 5]. Since it's easy to maintain the oxidation state of Th(IV), studies of tetravalent actinides using Th(IV) have apparent advantage.

Unfortunately, there is very limited data on the complexation of Th(IV) with EDTA [6, 7]. The existing data indicate that a combination of monomeric (ThEDTA(aq), $ThOHEDTA^-$) and dimeric species ($Th_2(OH)_2(EDTA)_2^{2-}$) is likely to be present in aqueous solutions. However, in a recent study on Pu(IV) complexation with EDTA Rai *et al.* [3] hypothesized only the formation of monomeric species. Since the studies of Rai *et al.* [3] on Pu(IV)-EDTA system

*Author for correspondence (E-mail: yuanxian.xia@pnl.gov).

were conducted in relatively dilute electrolyte solutions, the extension of these conclusions to concentrated electrolyte solutions is uncertain. Data are available on the solubility of Th(IV) hydrous oxides in the presence of NaCl [8–11]. However, no data are available on the solubility of Th(IV) hydrous oxide in high ionic strength electrolytes in the presence of chelates (such as EDTA).

With these factors in mind, this study was undertaken to determine the solubility of Th(IV) hydrous oxide 1) as a function of pC_{H^+} (ranging from 5 to 13) in varying concentrations of $NaNO_3$ (from 0.5 M to 6.0 M) at a fixed 0.01 M EDTA concentration, 2) at varying concentrations of EDTA ranging from 1.0×10^{-5} M to 1.0×10^{-2} M at a fixed pC_{H^+} values of 8 and 10 in 0.5 M $NaNO_3$. Based on these data we propose a thermodynamic model that describes the complexation reactions of Th(IV) with EDTA under basic conditions which is valid to high ionic strength. The results of this study are contrasted with the previous work on Pu(IV)-EDTA.

Experimental

Reagents and solutions

All reagents used in this study were analytical and reagent grade. All solutions were prepared with distilled-deionized (DDI) water and stored under an argon atmosphere. The thorium stock solution (1 M) used in this study was prepared by dissolving 552 g of reagent grade $Th(NO_3)_4 \cdot 4H_2O$ in 1 liter 0.1 M HNO_3. A standard CO_2-free NaOH solution (6.45 M) was prepared by dissolving a calculated amount of solid NaOH (Anachemia Acculute) and titrating it with standard HCl solution (6.0 M). The HCl solution (6.0 M) and concentrated HNO_3 were obtained from GFS Chemicals Inc. Stock solutions of 1.0 M EDTA and 6.5 M $NaNO_3$ were prepared by dissolving solids Na_4EDTA (Aldrich) and $NaNO_3$ (Baker Analyzed Reagent) in DDI water, respectively.

Procedures

All experiments were conducted at room temperature ($23 \pm 2\,^{\circ}C$) in a controlled argon gas chamber (99.99%, with < 1 ppm O_2). The solubilities of Th(IV) hydrous oxide (ThO_2(am)) in all experiments were approached from the undersaturation direction.

ThO_2(am) was precipitated by adding an aliquot of the thorium nitrate stock solution to 15 mls of water and adjusting the pH to about 10.5 using the NaOH stock solution. The resulting suspensions were centrifuged and the supernatant discarded. Soluble nitrate and sodium were removed by washing twice with 15 ml aliquots of water.

Seven sets of experiments were conducted with the washed ThO_2(am) precipitates (Table 1) to determine the solubility of ThO_2(am) as a function of pC_{H^+}, $NaNO_3$ concentration, EDTA concentration, and time. The general procedure consisted of suspending ThO_2(am) solids in 30 ml of appropriate EDTA/$NaNO_3$ solutions in centrifuge tubes, equilibrating the suspensions for different periods, separating the solids from suspensions, and analyzing the aqueous and/or solid phases. The pH values of suspensions were adjusted using NaOH and HCl. During the equilibration period the tubes were capped tightly and placed on a shaker in an argon gas chamber.

The solutions were sampled at the time intervals shown in Table 1. At these sampling intervals, the pH was measured with a Corning pH/ion 450 meter equipped with an Orion–Ross combination glass electrode calibrated against standard pH buffers. The pH meter readings (pH_{obs}) for the concentrated $NaNO_3$ solutions were converted to the hydrogen ion concentration ($pC_{H^+} = -\log[H^+]$) using the equation:

$$pC_{H^+} = pH_{obs} + A,$$

where A is the conversion factor that depends primarily on the solution composition. The values of A for the $NaNO_3$ solutions were determined to be -0.037 for 0.5 M $NaNO_3$, 0.315 for 3.0 M $NaNO_3$ and 0.752 for 6.0 M, respectively, using a titration method developed in previous studies [12].

Aliquots of the suspensions were centrifuged at 2000 g for 10 minutes. The supernatant was filtered through Amicon Centricon filters (Amicon Corp.) with a 30 000 molecular-weight cutoff and approximately 0.004 μm pore size. An aliquot (~ 1 ml) of the sample was passed through the filters (to saturate any possible adsorption sites) and discarded before the solution was filtered for analyses. The filtrate was acidified with HNO_3. An aliquot of acidified filtrate was taken for 1) the total thorium analysis by inductively coupled plasma spectroscopy (ICP) or inductively coupled plasma mass spectroscopy (ICP-MS), and 2) structure analysis of Th(IV)-chelates using X-ray absorption spectroscopy for selected samples containing relatively high concentrations of Th.

Table 1. A list of experiments conducted in this study.

Set number	Solid phase	pC_{H^+} range[c]	$NaNO_3$ (M)	EDTA (M)	Equilibration periods (days)
Set I	ThO_2(am)[a]	4.3 to 11.8	0.5	0.01	13, 31, 75
Set II	ThO_2(am)[a]	6.7 to 12.8	3.0	0.01	13, 30
Set III	ThO_2(am)[a]	6.8 to 13.2	6.0	0.01	13, 30
Set IV	ThO_2(am)[a]	8	0.5	10^{-5}–10^{-2}	8, 31
Set V	ThO_2(am)[a]	10	0.5	10^{-5}–10^{-2}	8, 31
Set VI	ThO_2(am)[b]	8	0.5	10^{-5}–10^{-2}	8, 31
Set VII	ThO_2(am)[b]	10	0.5	10^{-5}–10^{-2}	8, 31

a: The total approximate amounts of thorium solid phase used in each sample from sets were 100 mg in 30 ml solution;
b: The total approximate amounts of thorium solid phase used in each sample from sets were 10 mg in 30 ml solution;
c: $pC_{H^+} = pH_{obs} + A$ (see below).

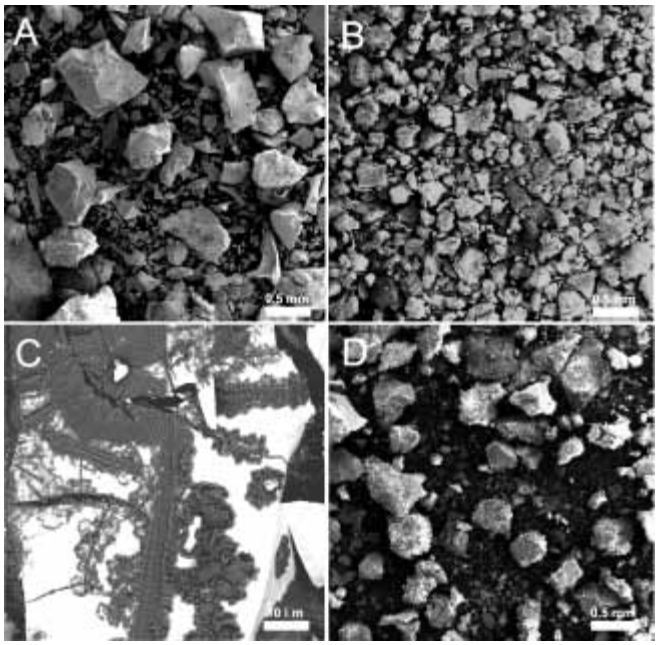

Fig. 1. SEM images of ThO_2(am)-solid samples equilibrated in 3.0 M $NaNO_3$ and twice rinsed with DDI water after centrifugation. A) No EDTA, pH 8.7, 3 hr equilibration time; B) and C) [EDTA] = 0.01 M, pH 8.7, 3 hr equilibration time; D) [EDTA] = 0.01 M, pH 8.9, 55 day equilibration time.

In addition, aliquots of the supernatants were directly taken (without filtration) for carbon analysis, and selected solids were characterized by scanning electron microscopy (SEM) and X-ray diffraction (XRD) after thoroughly rinsing with DDI water to remove the electrolyte.

The SEM and XRD analysis showed that the initial precipitates exhibited a wide range of particles sizes, some as large as 0.5 mm (Fig. 1a). Addition of the EDTA chelate to these samples resulted in rapid etching of all of the particles. After only three hours of equilibration the reaction of EDTA with the particle surfaces was evident mainly at the edges and fractures (Fig. 1c) but eventually extended to the entire particle. There was no evidence for the selective dissolution of only very fine particles. X-ray diffraction analyses indicated that the solid phases before and after equilibration with solutions are amorphous.

Extended X-ray Absorption Fine Structure (EXAFS) spectroscopy

EXAFS experiments were conducted with ThO_2(s), a solution of Th(IV) in perchloric acid ($[Th^{4+}] = 0.05$ M and $[HClO_4] = 1.0$ M), and two solutions of Th(IV) in the presence of EDTA from the solubility experiments. The concentrations of the two Th/EDTA solutions are: [Th(IV)] ~ 0.036 M, [EDTA] = 0.1 M, $pC_{H^+} = 8.18$; [Th(IV)] 0.007 M, [EDTA] = 0.01 M, $pC_{H^+} = 5.98$.

Thorium L_{III}-edge EXAFS spectra were collected at the Stanford Synchrotron Radiation Laboratory (SSRL) on wiggler beamline 4–1 under normal ring operating conditions (3.0 GeV, 50–100 mA). The EXAFS data were collected in the transmission mode, up to $k \sim 15$ Å^{-1}. Three to four scans were performed for each sample. Energy calibration was based on assigning the first inflection point of the absorption edge for thorium dioxide (ThO_2) to 16 300 eV. The EXAFS spectra were fitted using parameterized phase and amplitude functions generated by the program FEFF8 [13] with the reference crystal structures of ThO_2 and $Na_6Th(CO_3)_5(H_2O)_{12}$ [14]. Standard scattering paths, including the single scattering Th-O, Th-C and Th-Th were calculated from the reference structure and included in the data analysis.

Thermodynamic model

The aqueous thermodynamic model used in this study to interpret the solubility data was the ion-interaction model of Pitzer and coworkers [15, 16]. This model emphasizes a detailed description of the specific ion interactions in the solution. The effects of the specific ion interactions on the excess solution free energy are contained within the expressions for the activity coefficients. The activity coefficients can be expressed in a virial-type expansion as:

$$\ln \gamma_i^{DH} + \sum_j \beta_{ij}(I) m_j + \sum_j \sum_k C_{ijk} m_j m_k + \ldots , \qquad (1)$$

where m is the molality and γ_i^{DH} is a modified Debye–Hückel activity coefficient that is a universal function of ionic strength. $\beta_{ij}(I)$ and C_{ijk} are specific for each ion interaction and are a function of ionic strength. Pitzer gives explicit phenomenological expressions for the ionic-strength dependence of β. The third virial coefficient, C, is taken to be independent of ionic strength. The form of β is different for like, unlike, and neutral ion interactions. A detailed description of the exact form of Eq. (1) is given elsewhere [17–19]. The Pitzer thermodynamic model was used because it is applicable from zero to high concentration, and our solubility data extend to high ionic strength ($I \sim 7$ m).

Results and discussion

The solubility of ThO_2(am) is highly dependent on pC_{H^+} and the Th(IV) concentrations at different equilibration periods are similar, indicating that equilibrium, or at least steady-state concentrations are reached in < 13 days (Figs. 2–4). As expected, these observed solubilities are also several orders of magnitude greater than previously reported values obtained using the same solid material (ThO_2(am)), at similar ionic strength (0.6 M), but in the absence of strong organic chelates [8] (see Fig. 2 open squares). The concentrations of Th(IV) are nearly constant at $pC_{H^+} < 8.5$ and decrease with an increase in pC_{H^+} (Figs. 2–4). The nearly constant concentrations below $pC_{H^+} < 8.5$ are the result of nearly complete saturation of the 0.01 M EDTA solutions with Th(IV). The observed solubilities also do not show dramatic changes with changing electrolyte concentration from 0.5 M to 6.0 M $NaNO_3$ at the same pC_{H^+} value.

The solubilities are essentially at a 1 : 1 stoichiometric saturation with the measured chelate concentration below pC_{H^+} 8.5 indicating the presence of a 1 : 1 Th : EDTA species over this pC_{H^+} region. It is therefore of interest to compare these observed solubilities with predicted solubilities using existing thermodynamic models. In these initial thermodynamic modeling calculations, we utilized the sta-

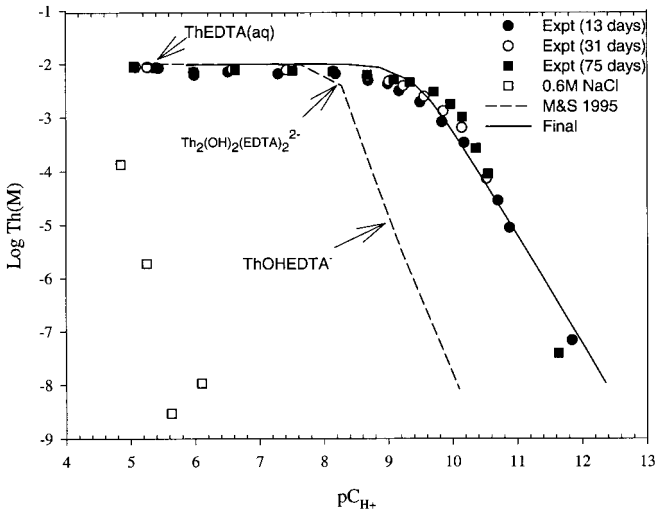

Fig. 2. ThO_2(am) solubilities in 0.5 M $NaNO_3$ as a function of pC_{H^+}. [EDTA] = 0.01 M. Data in 0.6 M NaCl from Felmy *et al.* [8]. The label M&S refers to calculations using the stability constants from Martell and Smith [6]. In this and subsequent figures, the label "final" refers to calculations using the final model parameters in Tables 2 and 3.

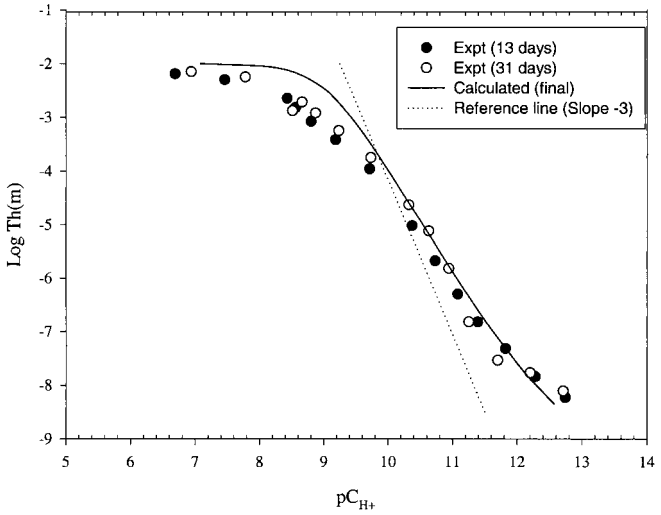

Fig. 3. ThO_2(am) solubilities in 3.0 M $NaNO_3$ as a function of pC_{H^+}. [EDTA] = 0.01 M. The dashed line with a slope of −3 is a reference line that would best represent the possible existence of a $ThOHEDTA^-$ species, see text.

bility constants critically reviewed by Martell and Smith [6] for Th-EDTA species (*i.e.*, ThEDTA(aq), $ThOHEDTA^-$, and $Th_2(OH)_2(EDTA)_2^{2-}$) with our [8] previously determined solubility product of ThO_2(am) prepared by the same methodology as used in this study. The predicted solubilities (see dashed line in Fig. 2) agree well with the experimental data up to a pC_{H^+} value of approximately 8.5, whereupon the predicted solubilities are considerably lower than the experimental values. Interestingly, pC_{H^+} 8.5 is also near the upper limit of the original EMF measurements made by Bogucki and Martell [7], which is the original source of the recommended stability constants for the ThEDTA(aq), $ThOHEDTA^-$, and $Th_2(OH)_2(EDTA)_2^{2-}$ species (see Bogucki and Martell [7], Fig. 1).

There are several possible explanations for the disagreement between the initial model calculations and the experimental values. First, the ionic strength of the solutions is somewhat greater (0.5 M) than the ionic strength at which the stability constants were determined (0.1 M) and this could result in some of the disagreement. However, the principal species predicted to be present at high concentration is the singly charged $ThOHEDTA^-$ species. Species of such low charge rarely have large ionic strength dependence relative to more highly charged species. In addition, the observed ionic strength changes from 0.5 M to 6.0 M do not result in an large change in the observed Th concentrations. It is therefore unlikely that a large ionic strength effect occurs on the stability constants between 0.1 M and 0.5 M. In addition, a preliminary fit of the experimental data to the observed solubilities in 0.5 M $NaNO_3$, by adjusting the stability constant for the $ThOHEDTA^-$ species, showed that the stability constant would need to increase by five log units to begin to match the experimental values. Such a large change in stability is not the result of ionic strength changes. This large change in stability is also unlikely to result from errors in the original EMF analysis of Bogucki and Martell [7] since their data appears to be very precise and the disagreement occurs only in the higher pC_{H^+} region. This pC_{H^+} region was not investigated by Bogucki and Martell [7]. It is also possible that the solubility product for the ThO_2(am) used in these preliminary calculations (see Table 1) is considerably different from the value for the actual material. However, the solubility product that was used in these calculations was originally calculated from the low ionic strength data of Ryan and Rai [20] by Felmy *et al.* [8] and thoroughly tested against data in $NaClO_4$ and NaCl by Felmy *et al.* [8] and again by Rai *et al.* [10] in NaCl and $MgCl_2$. This value $\log K = -45.5$ is also in good agreement with the recommended value of Martell and Smith [6] (−44.7) especially when it is realized that a value approximately five orders of magnitude more soluble (*i.e.* $\log K \sim 40.5$) would be required to even partially explain the observed differences, assuming the current aqueous speciation scheme is valid. Changes of five orders of magnitude are found between crystalline and amorphous material. For example, Martell

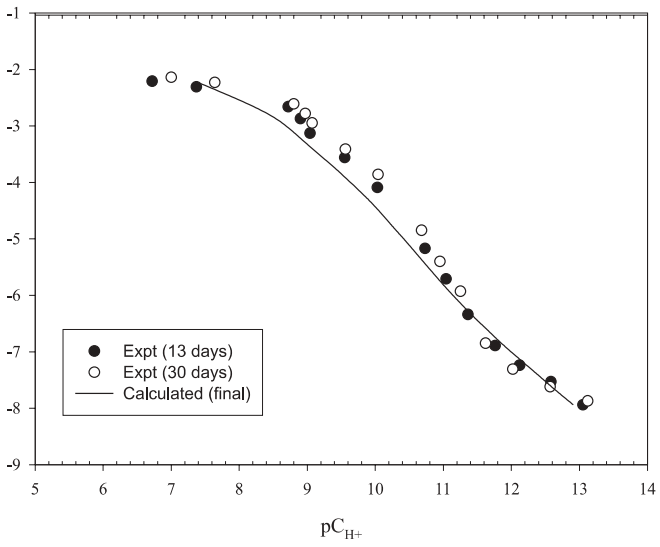

Fig. 4. ThO_2(am) solubilities in 6.0 M $NaNO_3$ as a function of pC_{H^+}. [EDTA] = 0.01 M. The final calculated line utilizes the Pitzer ion-interaction parameters and stability constants in Tables 2 and 3.

and Smith [6] recommended $\log K = -49.7$ for ThO_2(c), but the use of a more crystalline value for the solubility product would only further increase the difference between model calculations and experimental data. We therefore conclude that the observed differences between calculated and experimental solubilities are the result of the neglect of additional Th-EDTA aqueous species for which the stability constants have not been determined.

Recent studies of Pu(IV)-EDTA complexation reactions under neutral to basic conditions [3] have indicated the presence of only monomeric species (*i.e.*, $PuOHEDTA^-$, $Pu(OH)_2EDTA^{2-}$, and $Pu(OH)_3EDTA^{3-}$). Assuming there is some analogy between Pu(IV) and Th(IV), these conclusions would indicate that Th(IV) species such as $Th(OH)_2EDTA^{2-}$, and/or $Th(OH)_3EDTA^{3-}$ could be present. However, the studies of Bogucki and Martell [7] did show clear indications of dimerization reactions in their EMF data, so the presence of higher order species (dimers, trimers, ...) cannot be ruled out a prior.

In order to further investigate these issues we conducted studies at different aqueous EDTA concentrations, studies in the presence of different amounts of solid ThO_2(am), and performed X-Ray absorption analysis on selected samples at the Stanford Synchrotron Radiation Laboratory.

In the case of the XAS analysis, the majority of the samples in the higher pC_{H^+} range were too low in concentration to obtain any useful information. We therefore also prepared a sample at higher EDTA concentration (0.1 M) in an effort to help identify the species present. Of the selected samples sent for analysis, definitive EXAFS spectra were obtained for only two samples. The Fourier Transform magnitude of the EXAFS is shown in Fig. 5 (the bottom two plots). EXAFS spectra of two references samples were also collected: a strongly acidic $Th(ClO_4)_4$ solution, where there should be no neighboring Th atoms; and a ThO_2(s) sample which shows the positions of the Th-Th backscatter. The results for these two references are shown as the top two plots in Fig. 5. Standard scattering paths of Th-O, Th-Th are used in the fits. The error limits for the number of the atom are ±25%. It can be seen that there are no features in the two samples ($pC_{H^+} = 5.98$, EDTA = 0.01 M and $pC_{H^+} = 8.18$, EDTA = 0.1 M) that could be fit with a Th-Th scattering. We therefore conclude that at least in these two samples dimeric or higher Th-EDTA complexes are not present in significant concentration. The result for the 0.1 M EDTA sample is especially significant since such high Th containing samples (Th = 0.03 M) are the more likely ones to exhibit dimerization reactions than lower concentration samples. This is another indication that the unknown aqueous species present are monomeric.

The results for the studies at different EDTA concentration are shown in Figs. 6 and 7. These samples were adjusted

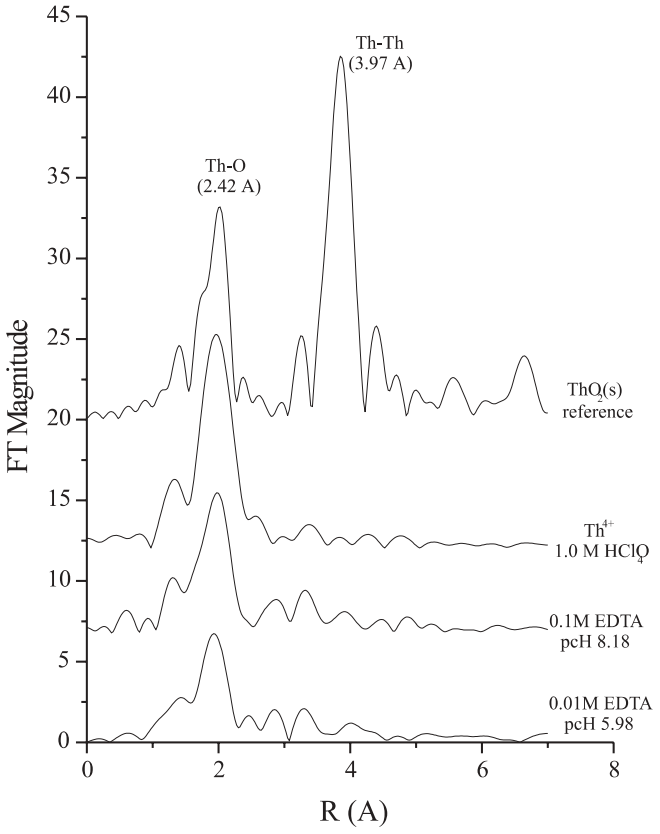

Fig. 5. Fourier transform magnitude of the EXAFS spectra of Th(IV) in ThO_2(s), 1.0 M $HClO_4$, 0.1 M EDTA and 0.01 M EDTA.

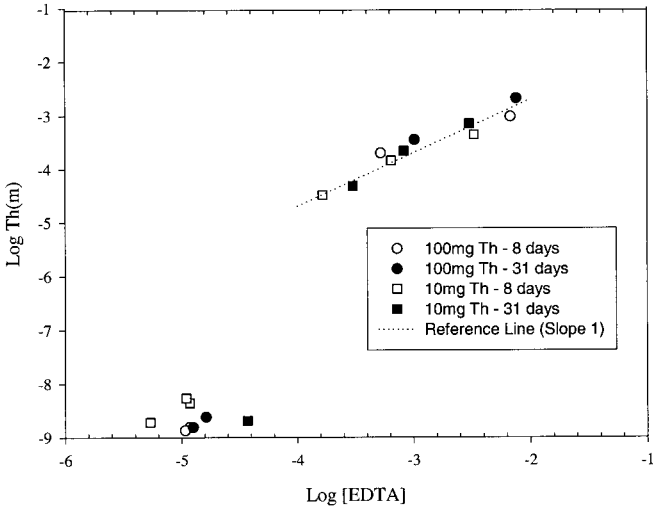

Fig. 6. ThO_2(am) solubilities as a function of chelate concentration and added ThO_2(am) at a pC_{H^+} of approximately 8.

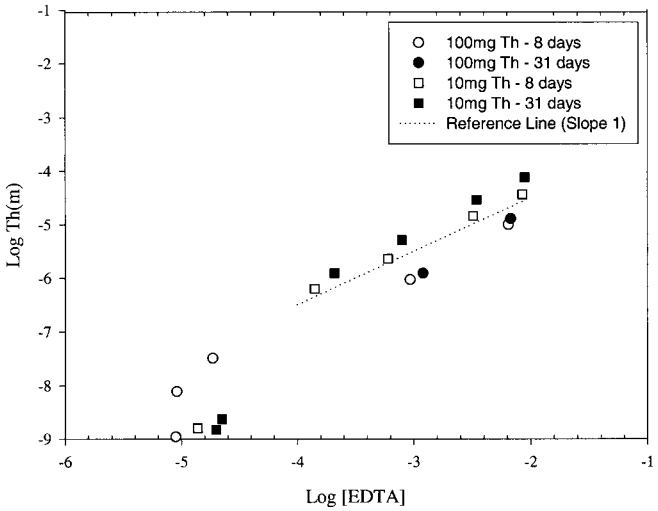

Fig. 7. ThO_2(am) solubilities as a function of chelate concentration and added ThO_2(am) at a pC_{H^+} of approximately 10.

to obtain as constant a pC_{H^+} value as possible (the exact data is reported in the Appendix). The data in Fig. 6 were all near pC_{H^+} 8 and the data in Fig. 7 are all near pC_{H^+} 10. The results show some interesting features. First, the aqueous Th concentrations increase linearly with added EDTA above concentrations of 10^{-4} M. This increase is consistent at both pC_{H^+} 8 and pC_{H^+} 10. This linear increase with a slope of one is another strong indication that monomeric complexes dominate the aqueous speciation. However, at lower EDTA concentrations there is an abrupt drop in the dissolved Th concentrations. This abrupt drop is directly related to an absence of chelate from the solutions. The disappearance of chelate is shown in Fig. 8 where it can be readily seen that in solution containing 100 mg Th as ThO_2(am) essentially all of the EDTA is adsorbed to the solid phase at added EDTA concentrations of $< 10^{-3}$ M. In solutions with only 10 mg Th as ThO_2(am) complete adsorption of the chelate occurs at about 10^{-4} M. So there is a clear adsorption maximum for EDTA onto ThO_2(am) and adsorption maximum appears to be independent of pH (at least between pH 8 and 10).

It is unclear whether this adsorption of chelate could have influenced previous solubility studies of tetravalent actinides in the presence of EDTA. Rai *et al.* [3] working with PuO_2(am) and EDTA did not report chelate adsorption, yet their calculated Pu(IV) concentrations were two orders of magnitude higher than experimentally observed at chelate concentrations of $\leq 10^{-4}$ M added EDTA and in the presence of 2 mg Pu as PuO_2(am) (see Fig. 6 in Rai *et al.* [3]). Rai *et al.* [3] did not report their method of analysis of EDTA, or in fact whether or not the final EDTA concentrations were measured. Regardless, the adsorption of EDTA certainly occurs in the case of ThO_2(am). This fact places certain constraints on the EDTA concentrations that can be explored by the solubility method. If the chelate concentration is too low, adsorption of EDTA dominates and little thermodynamic information can be gained about aqueous speciation. If the EDTA concentration relative to the amount of ThO_2(am) is too high, then all of the precipitate dissolves and no equilibrium can be maintained. As a result our following thermodynamic analysis emphasized the data in 10^{-2} M EDTA solutions shown in Figs. 2–4. Some adsorption of EDTA did occur in these solutions but our selected analysis of the EDTA, as well as the data shown in Fig. 8, indicate that the vast majority of the chelate remained in solution in these studies.

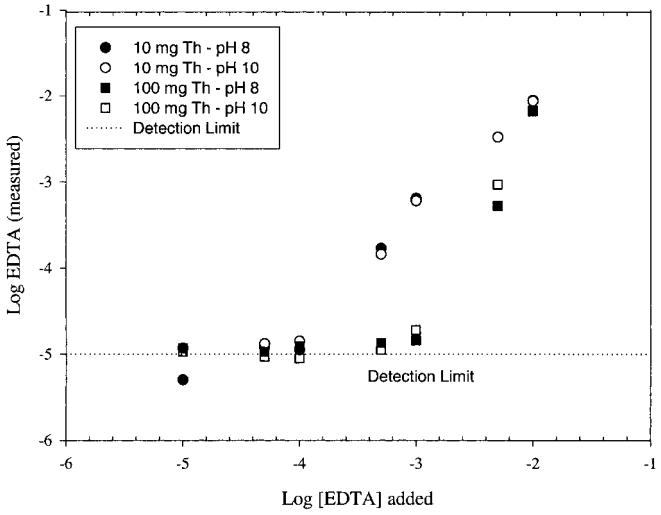

Fig. 8. Experimentally observed EDTA concentrations as a function of the amount of added EDTA. Differences between added and measured values are an indication of the amount adsorbed by the solid phase ThO_2(am).

In summary, all of the lines of evidence that we have, including XAS analysis, ThO_2 solubilities as a function of chelate concentration, the relatively low total Th concentrations in the higher pC_{H^+} region, and the previous results for Pu(IV)-EDTA [3] all point to monomeric Th-EDTA complexes as the predominant species present at higher pC_{H^+} regions. It is unlikely that either of the previously defined monomeric species (ThEDTA(aq) or $ThOHEDTA^-$) are the likely species present since their previously reported stability constants would need to be in error by several log units. It also became apparent in initial fits to the experimental data that these two species did not give the best fits to the data at all three $NaNO_3$ concentrations. The reasons for these generally poor fits can be seen when the reactions between amorphous ThO_2(am) and the various monomeric species are written,

$$ThO_2(am) + 4H^+ + EDTA^{4-} \leftrightarrow ThEDTA(aq) + 2H_2O\,, \quad (2)$$

$$ThO_2(am) + 3H^+ + EDTA^{4-} \leftrightarrow ThOHEDTA^- + H_2O\,, \quad (3)$$

$$ThO_2(am) + 2H^+ + EDTA^{4-} \leftrightarrow Th(OH)_2EDTA^{2-}\,, \quad (4)$$

$$ThO_2(am) + H^+ + EDTA^{4-} + H_2O \leftrightarrow Th(OH)_3EDTA^{3-}\,. \quad (5)$$

If visualized in the form of plots of log Th *versus* pC_{H^+} reactions Eqs. (2)–(5) should have slopes of -4, -3, -2, and -1 respectively. The analysis of the data, especially at $NaNO_3$ concentrations of 3.0 M and 6.0 M, shows that reactions Eq. (4) and Eq. (5) give the best overall fits. The inability of reactions Eq. (2) or Eq. (3) to explain the results is indicated by the dashed line in Fig. 3, which shows that a slope of -3 (reaction (3)) will not give a very good representation of the results. In fact, the majority of the data can be readily explained simply by assuming the existence of the $Th(OH)_2EDTA^{2-}$ species. Only the limited data in 3.0 M $NaNO_3$ and 6.0 M $NaNO_3$ above a pC_{H^+} value of 12 require the introduction of the $Th(OH)_3EDTA^{3-}$ species. Therefore, the assumptions as to the existence of this latter species should be considered as tentative.

With these thoughts in mind, the best fits to the experimental data yield equilibrium constants for the following reactions,

$$ThO_2(am) + EDTA^{4-} + 2H_2O \leftrightarrow Th(OH)_2EDTA^{2-} + 2OH^-, \quad \log K = -6.0 \quad (6)$$

and,

$$ThO_2(am) + EDTA^{4-} + 2H_2O \leftrightarrow Th(OH)_3EDTA^{3-} + OH^-, \quad \log K \sim -7.5\,. \quad (7)$$

In addition, Pitzer ion-interaction parameters for the $Th(OH)_2EDTA^{2-}$ and $Th(OH)_3EDTA^{3-}$ species were re-

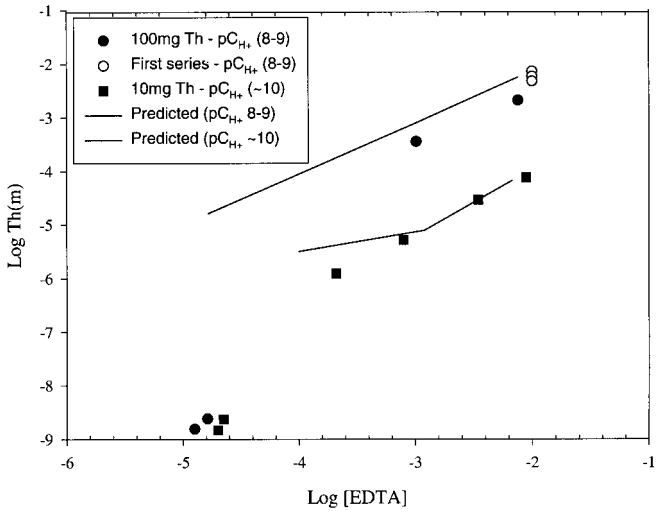

Fig. 9. Experimental and calculated ThO_2(am) solubilities in samples as a function of added EDTA. Calculations assume the pC_{H^+} values and EDTA concentrations for the 31 day, 100 mg Th samples at $pC_{H^+} \sim 8$ and the 10 mg, 31 day values at $pC_{H^+} \sim 10$. The terminology "first series" refers to the data between pC_{H^+} 8 and 9 shown in Fig. 2.

quired to describe the $NaNO_3$ dependence of the solubility reactions. These ion-interaction parameters were β^0 (Na^+–$Th(OH)_2EDTA^{2-}$) = 0.64 and β^0 (Na^+–$Th(OH)_3EDTA^{3-}$) = 0.53. This model yields the final predictions shown in Figs. 2–4, solid lines. It can be seen that the agreement between model and experiment is quite good.

This model was also used to predict the solubilities as a function of EDTA concentration at pC_{H^+} values of ~ 8 and 10, solid lines Fig. 9. These calculations needed to be performed for each individual data set owing to the variabilities in pC_{H^+} values for the samples shown in Figs. 6 and 7. The results show good agreement between the model calculations and experimental points. The calculated curve for the samples at $pC_{H^+} \sim 10$ shows an upturn for the lower EDTA concentration data. This is due to a lower pC_{H^+} value for these samples which results in a higher predicted Th concentration.

It is also of interest to rewrite reactions Eq. (6) and Eq. (7) in terms of aqueous association reactions,

$$Th^{4+} + 2OH^- + EDTA^{4-} \leftrightarrow Th(OH)_2EDTA^{2-}, \quad \log K = 39.5, \tag{8}$$

$$Th^{4+} + EDTA^{4-} + 3OH^- \leftrightarrow Th(OH)_3EDTA^{3-}, \quad \log K \sim 38.0, \tag{9}$$

assuming a solubility product for ThO_2(am) of −45.5 as previously described. The equilibrium constants for reactions Eq. (8) and Eq. (9) compare with similar reactions proposed by Rai *et al.* [3] for the corresponding Pu(IV) species which have LogK values of 44.8 and 49.8 respectively. As expected, the association reactions for Th(IV) are not as strong as for Pu(IV). The fact that the observed solubilities for ThO_2(am) are considerably higher than for PuO_2(am) in EDTA-containing solutions results from the differences in solubility products for ThO_2(am) and PuO_2(am) (*i.e.*, −45.5 *versus* −56.9) not stronger Th(IV)-EDTA complexation.

The differences in association between the $Pu(OH)_2$-$EDTA^{2-}$ species and the $Pu(OH)_3EDTA^{3-}$ species (5 log units) is considerably more than that calculated in this study for the corresponding Th(IV) species. These differences in stability result from differences in assumptions during the mathematical fitting procedure. In our case the "formation" of the $Th(OH)_3EDTA^{3-}$ species results solely from changes in $NaNO_3$ concentration (compare Figs. 2, 3, and 4) at similar pC_{H^+} values. If correct, such changes are not due to a greatly enhanced intrinsic stability of the $Th(OH)_3EDTA^{3-}$ species but more to stronger association of the Na^+ cations with the more highly charged $Th(OH)_3EDTA^{3-}$ species, which shifts the equilibria toward this species. In the case of the Pu(IV) species the stabilities were not examined as a function of ionic strength but were estimated solely from perceived changes in slope as a function of pH. Additional studies of Pu(IV)-EDTA as a function of electrolyte composition would be required to evaluate if the Pu(IV)-EDTA system responds in the same fashion as the Th(IV)-EDTA system.

The Pitzer ion-interaction parameters utilized in this study are summarized in Table 2 and the standard state equilibrium constants are in Table 3. In the case of the Pitzer

Table 2. Pitzer ion-interaction parameters used in this study.

Species	Parameter	Value (25 °C)	Reference
Na^+-OH^-	β^0	0.0868	Felmy and Mason [21]
	β^1	0.253	"
	C^ϕ	0.00415	"
Na^+-$EDTA^{4-}$	β^0	1.1	"
	β^1	15.6	"
	C^ϕ	0.001	Mizera *et al.* [22]
Na^+-$NaEDTA^{3-}$	β^0	0.59	Felmy and Mason [21]
	β^1	5.39	"
Na^+-$Th(OH)_2EDTA^{2-}$	β^0	0.64	This Study
Na^+-$Th(OH)_3EDTA^{3-}$	β^0	0.53	"
Na^+-Th^{4+}	θ	0.42	Felmy and Rai [23]
Th^{4+}-NO_3^-	β^0	0.966	Pitzer [16]
	β^1	11.4	"
	C^ϕ	−0.185	"
OH^--NO_3^-	θ	−0.00005	Felmy *et al.* [24]
NO_3^--$NaEDTA^{3-}$	θ	0.12	Felmy and Mason [21]

Table 3. Logarithms (base 10) of the thermodynamic equilibrium constants of aqueous phase association reactions and solid phase dissolution reactions used in this study.

Species	log *K*	Reference
$NaEDTA^{3-}$	2.70	Felmy and Mason [21]
ThEDTA(aq)	23.2	Martell and Smith [6]
$ThOHEDTA^{-}$	30.2	"
$Th(OH)_2EDTA^{2-}$	39.5	This Study
$Th(OH)_3EDTA^{3-}$	38.0	"
$ThO_2(am)$	−45.5	Felmy *et al.* [8]
$NaNO_3(aq)$	−1.04	Felmy *et al.* [24]

ion-interaction parameters we have chosen to utilize our latest set of values for Na^+-$EDTA^{4-}$ interactions that also includes the formation of a $NaEDTA^{3-}$ species. These parameters were developed from an extensive set of solubility and apparent equilibrium constant data [21]. They are also consistent with previous NMR measurements that show the strong binding of the Na^+ ion to the EDTA chelate. However, it is worth nothing that if previously accepted model for Na^+-$EDTA^{4-}$ interactions are used [22] which are based solely upon the use of Pitzer ion-interaction parameters, the final calculated solubilities are essentially identical to the predictions shown in Figs. 2–4 and the calculated stability constants for Th-EDTA species change by only 0.3 to 0.4 log units. For example, the calculated stability constant for reaction Eq. (8) would change from 39.5 to 39.1. We have elected to retain our currently proposed thermodynamic model for Na^+-$EDTA^{4-}$ interactions owing to the wide range of experimental data that were used in the analysis.

Acknowledgment. This research was supported by the Department of Energy Environmental Management Sciences Program (EMSP) under the project entitled "Chemical Speciation of Strontium, Americium, and Curium in High-Level Waste: Predictive Modeling of Phase Partitioning During Tank Processing" Project No. 26753. We thank B.W. Arey for the SEM analysis. Pacific Northwest National Laboratory is operated by Battelle for the United States Department of Energy under Contract DE-AC06-76RL01830.

Appendix

Table A1. Aqueous Th concentrations from $ThO_2(am)$ in 0.5 M $NaNO_3$ and 0.01 M EDTA.

	13 days			31 days			75 days	
pH_{obs}	pC_{H^+}	log [Th] (M)	pH_{obs}	pC_{H^+}	log [Th] (M)	pH_{obs}	pC_{H^+}	log [Th] (M)
			4.371	4.334	−1.964	4.359	4.322	−2.030
5.117	5.080	−2.060	5.118	5.081	−2.046	5.092	5.055	−2.040
5.315	5.278	−2.062	5.296	5.259	−2.059	5.098	5.061	−2.061
5.473	5.438	−2.078	5.440	5.403	−2.067	5.442	5.405	−2.073
6.027	5.990	−2.208	6.019	5.983	−2.153	6.015	5.976	−2.153
6.549	6.512	−2.146	6.617	6.580	−2.100	6.663	6.626	−2.117
7.328	7.291	−2.185	7.458	7.421	−2.113	7.551	7.514	−2.129
8.220	8.183	−2.186	8.186	8.149	−2.141	8.183	8.146	−2.145
8.727	8.690	−2.312	8.715	8.678	−2.237	8.713	8.676	−2.206
9.022	8.995	−2.377	9.049	9.012	−2.327	9.128	9.091	−2.296
9.208	9.171	−2.507	9.274	9.237	−2.412	9.376	9.339	−2.346
9.533	9.496	−2.716	9.597	9.560	−2.611	9.746	9.709	−2.526
9.873	9.836	−3.079	9.891	9.854	−2.882	10.007	9.970	−2.754
10.216	10.179	−3.468	10.182	10.145	−3.188	10.186	10.149	−2.991
10.737	10.700	−4.546	10.559	10.522	−4.136	10.399	10.362	−3.569
10.918	10.881	−5.057	10.956	10.919	−4.744	10.586	10.549	−4.040
11.879	11.842	−7.168	11.788	11.751	−7.211	11.671	11.634	−7.412

Table A2. Aqueous Th concentrations from $ThO_2(am)$ in 3.0 M $NaNO_3$ and 0.01 M EDTA.

	13 days			30 days	
pH_{obs}	pC_{H^+}	log [Th] (M)	pH_{obs}	pC_{H^+}	log [Th] (M)
6.432	6.747	−2.251	6.689	7.004	−2.214
7.200	7.515	−2.367	7.533	7.848	−2.308
8.182	8.497	−2.709	8.257	8.572	−2.940
8.305	8.620	−2.892	8.402	8.717	−2.780
8.541	8.856	−3.140	8.615	8.930	−2.984
8.926	9.241	−3.482	8.974	9.289	−3.313
9.459	9.774	−4.032	9.477	9.792	−3.806
10.120	10.435	−5.097	10.066	10.381	−4.690
10.480	10.795	−5.741	10.381	10.696	−5.182
10.823	11.138	−6.358	10.682	10.997	−5.870
11.138	11.463	−6.866	10.992	11.307	−6.876
11.563	11.878	−7.379	11.442	11.757	−7.602
12.027	12.342	−7.913	11.950	12.266	−7.838
12.485	12.800	−8.295	12.457	12.772	−8.171

Table A3. Aqueous Th concentrations from ThO_2(am) in 6.0 M $NaNO_3$ and 0.01 M EDTA.

pH_{obs}	13 days pC_{H^+}	log [Th] (M)	pH_{obs}	30 days pC_{H^+}	log [Th] (M)
6.066	6.818	−2.306	6.346	7.098	−2.244
6.721	7.473	−2.410	6.992	7.744	−2.320
8.072	8.824	−2.758	8.145	8.897	−2.714
8.242	8.994	−2.978	8.319	9.071	−2.881
8.388	9.140	−3.230	8.415	9.167	−3.055
8.895	9.647	−3.670	8.907	9.659	−3.509
9.380	10.132	−4.207	9.384	10.136	−3.956
10.080	10.832	−5.270	10.027	10.779	−4.948
10.382	11.134	−5.806	10.299	11.051	−5.500
10.711	11.463	−6.436	10.593	11.345	−6.033
11.106	11.858	−6.989	10.966	11.757	−6.947
11.468	12.220	−7.340	11.362	12.114	−7.411
11.925	12.677	−7.631	11.916	12.668	−7.723
12.393	13.145	−8.042	12.466	13.218	−7.970

Table A4. Aqueous Th concentrations from ThO_2(am) in 0.5 M $NaNO_3$ and varying concentrations of EDTA at a fixed pC_{H^+} 10.

log [EDTA][a] (M)	pC_{H^+}	log [Th] 8 days (M)	log [EDTA][a] (M)	pC_{H^+}	log [Th] 31 days (M)
		(Equilibrated solution contacted with 10 mg ThO_2(am))			
−4.936	9.983	−9.204	−4.908	9.798	−9.727
−4.888	9.953	−9.185	−4.701	9.952	−8.834
−4.856	9.951	−8.802	−4.648	9.982	−8.630
−3.852	10.026	−6.203	−3.684	10.171	−5.914
−3.225	10.037	−5.635	−3.101	10.125	−5.292
−2.491	10.540	−4.839	−2.461	10.520	−4.540
−2.071	10.422	−4.441	−2.053	10.469	−4.116
		(Equilibrated solution contacted with 100 mg ThO_2(am))			
−4.976	9.816	−9.827	−4.925	9.868	−9.871
−5.038	9.967	−8.113	−4.956.	9.830	
−5.053	9.981	−8.957	−4.927	9.816	−9.862
−4.958	10.090		−4.792	9.898	−9.896
−4.733	10.119	−7.487	−4.740	9.896	−9.414
−3.035	10.514	−6.034	−2.924	10.520	−5.914
−2.191	10.462	−5.002	−2.169	10.409	−4.888

a: The concentrations of EDTA added into samples are analytical data based on the analytical results of carbon for each sample.

Table A5. Aqueous Th concentrations from ThO_2(am) in 0.5 M $NaNO_3$ and varying concentrations of EDTA at a fixed pC_{H^+} 8.

log [EDTA][a] (M)	pC_{H^+}	log [Th] 8 days (M)	log [EDTA][a] (M)	pC_{H^+}	log [Th] 31 days (M)
		(Equilibrated solution contacted with 10 mg ThO_2(am))			
−5.270	7.873	−8.722	−4.814	7.873	−9.605
−4.927	8.112	−8.360	−4.800	7.961	−9.255
−4.956	8.132	−8.270	−4.428	7.963	−8.691
−3.779	8.079	−4.493	−3.523	8.784	−4.317
−3.193	8.235	−3.843	−3.077	8.859	−3.661
−2.485	8.770	−3.359	−2.518	8.725	−3.152
		(Equilibrated solution contacted with 100 mg ThO_2(am))			
−4.938	7.974	−8.809	−4.901	7.823	−8.880
−4.974	8.056	−8.872	−4.955	8.009	−9.883
−4.920	8.062	−9.919	−5.040	8.028	−9.787
−4.881	8.664	−9.492	−4.764	7.944	−9.128
−4.848	8.643	−9.120	−4.785	8.158	−8.617
−3.290	8.563	−3.702	−2.989	8.995	−3.453
−2.180	8.418	−3.024	−2.122	9.064	−2.676

a: The concentrations of EDTA added into samples are analytical data based on the analytical results of carbon for each sample.

References

1. Felmy, A. R.: Thermodynamic Modeling of Sr/TRU Removal. PNWD-3044, BNFL-RPT-037 Rev 0 (2000).
2. Choppin, G. R., Bond, A. H., Borkowski, M., Bronikowski, M. G., Chen, J., Lis, S., Mizera, J., Pokrovsky, O., Wall, N. A., Xia, Y., Moore, R. C.: Waste Isolation Pilot Plant Actinide Source Term Test Program: Solubility Studies and Development of Modeling Parameters. SANDIA REPORT SAND99-0943 (2001).
3. Rai, D., Bolton, H., Jr., Moore, D. A., Hess, N. J., Choppin, G. R.: Thermodynamic model for the solubility of PuO_2(am) in the aqueous Na^+-H^+-OH^--Cl^--H_2O-ethylenediaminetetraactate system. Radiochim. Acta **89**, 67 (2001).
4. Katz, J. J., Morss, L. R., Seaborg, G. T.: *The Chemistry of the Actinide Elements*. Chapman and Hall, London (1986).
5. Xia, Y., Rao, L., Rai, D., Felmy, A. R.: Solvent extraction study of Np(IV) sulfate complexation in Na^+-Np^{4+}-OH^--SO_4^{2-}-HSO_4^--ClO_4^- and Na^+-Np^{4+}-OH^--SO_4^{2-}-HSO_4^--Cl^- systems. Radiochim. Acta **86**, 33 (1999).
6. Martell, A. E., Smith, R. M: Critically Selected Stability Constants of Metal Complexes Database. Version 2.0. NIST Standard Reference Data Program, Gaithersburg, MD (1995).
7. Bogucki, R. F., Martell, A. E.: Hydrolysis and olation of Th(IV) chelates of polyaminopolycarboxylic acids. J. Amer. Chem. Soc. **80**, 4170 (1958).
8. Felmy, A. R., Rai, D., Mason, M. J.: The solubility of hydrous thorium(IV) oxide in chloride media: development of an aqueous ion-interaction model. Radiochim. Acta **55**, 177 (1991).
9. Rai, D., Felmy, A. R., Moore, D. A., Mason, M. J.: The solubility of Th(IV) and U(IV) hydrous oxides in concentrated $NaHCO_3$ and Na_2CO_3 solutions. Mat. Res. Soc. Symp. Proc. Vol. **353**, Materials Research Society (1995).
10. Rai, D., Felmy, A. R., Sterner, S. M., Moore, D. A., Mason, M. J.: The solubility of Th(IV) and U(IV) hydrous oxides in concentrated NaCl and $MgCl_2$ solutions. Radiochim. Acta **79**, 239 (1997).
11. Rai, D., Moore, D. A., Charles, C. S., Yui, M.: Thermodynamic model for the solubility of thorium dioxide in the Na^+-Cl^--OH^--H_2O system at 23 °C and 90 °C. Radiochim. Acta **88**, 297 (2000).
12. Rai, D., Felmy, A. R., Juracich, S. P., Rao, L.: Estimating the Hydrogen Ion Concentrated NaCl and Na_2SO_4 Electrolytes. SAND94-1949, Sandia National Laboratory, Albuquerque, New Mexico (1995).
13. Zabinsky, S. I., Rehr, J. J., Ankudinov, A., Albers, R. C., Eller, M. J.: Multiple-scattering calculations of X-ray-absorption spectra. Phys. Rev. B. **52**, 2995 (1995).
14. Voliotis, S., Rimsky, A.: Etude Structurale des Carbonates Complexes de Cérium et de Thorium. III. Structure Cristalline et Moléculaire du Pentacarbonatothorate de Sodium Dodécahydraté, $Na_6[Th(CO_3)_5]\cdot 12H_2O$. Acta Cryst. B **31**, 2615 (1975).
15. Pitzer, K. S.: Thermodynamics of electrolytes. I. Theoretical basis and general equations. J. Phys. Chem. **77**, 268 (1973).
16. Pitzer, K. S.: Ion Interaction Approach: Theory and Data Correlation in Activity Coefficients. In: *Electrolyte Solutions*. 2nd edn., CRC Press, Boca Raton (1991) pp. 75–153.
17. Harvie, C. E., Moller, N., Weare, J. H.: The prediction of mineral solubilities in natural waters: the Na-K-Mg-Ca-H-Cl-SO_4-OH-HCO_3-CO_2-H_2O system to high ionic strengths at 25 °C. Geochim. Cosmochim. Acta **48**, 723 (1984).
18. Felmy, A. R., Weare, J. H.: The prediction of borate mineral equilibria in natural waters: application to Searles Lake, California. Geochim. Cosmochim. Acta **50**, 2771 (1986).
19. Felmy, A. R, Rai, D., Schramke, J. A., Ryan, J. I.: Solubility of plutonium hydroxide in dilute solution and in high-ionic strength chloride brines. Radiochim. Acta **48**, 29 (1989).
20. Ryan, J. L., Rai, D.: Thorium(IV) hydrous oxide solubility. Inorg. Chem. **26**, 4140 (1987).
21. Felmy, A. R., Mason, M. J.: An Aqueous Thermodynamic Model for the Complexation of Sodium and Strontium with Organic Chelates Valid to High Ionic Strength. I. Ethylenedinitrilotetraacetic acid (EDTA). J. Solution Chem. **32**(4), 283 (2003).
22. Mizera, J., Bond, A. H., Choppin, G. R., Moore, R. C.: Dissociation constants of carboxylic acids at high ionic strengths. In: *Actinide Speciation in High Ionic Strength Media*. (Reed *et al.*, eds.) Kluwer Academic/Plenum Publishers, New York (1999) pp. 113–124.
23. Felmy, A. R., Rai, D.: Application of Pitzer's equations for modeling the aqueous thermodynamics of actinide species: a review. J. Solution Chem. **28** 533 (1999), special memorial edition in honor of Professor Kenneth Pitzer.
24. Felmy, A. R., Rustad, J. R., Mason, M. J., de la Bretonne, R.: A Chemical Model for the Major Electrolyte Components of the Hanford Waste Tanks. TWRS-PP-94-090. Westinghouse Hanford Co. Richland, WA (1994).